Evidence for the prepattern/cooption model of vertebrate jaw evolution

Robert Cerny[a], Maria Cattell[b], Tatjana Sauka-Spengler[c], Marianne Bronner-Fraser[c], Feiqiao Yu[c], and Daniel Meulemans Medeiros[b,1]

[a]Department of Zoology, Charles University in Prague, 128 44 Prague, Czech Republic; [b]Department of Ecology and Evolutionary Biology, University of Colorado, Boulder, CO 80309; and [c]Division of Biology, California Institute of Technology, Pasadena, CA 91125

Edited by Clifford J. Tabin, Harvard Medical School, Boston, MA, and approved August 31, 2010 (received for review July 2, 2010)

The appearance of jaws was a turning point in vertebrate evolution because it allowed primitive vertebrates to capture and process large, motile prey. The vertebrate jaw consists of separate dorsal and ventral skeletal elements connected by a joint. How this structure evolved from the unjointed gill bar of a jawless ancestor is an unresolved question in vertebrate evolution. To understand the developmental bases of this evolutionary transition, we examined the expression of 12 genes involved in vertebrate pharyngeal patterning in the modern jawless fish lamprey. We find nested expression of *Dlx* genes, as well as combinatorial expression of *Msx, Hand* and *Gsc* genes along the dorso-ventral (DV) axis of the lamprey pharynx, indicating gnathostome-type pharyngeal patterning evolved before the appearance of the jaw. In addition, we find that *Bapx* and *Gdf5/6/7*, key regulators of joint formation in gnathostomes, are not expressed in the lamprey first arch, whereas *Barx*, which is absent from the intermediate first arch in gnathostomes, marks this domain in lamprey. Taken together, these data support a new scenario for jaw evolution in which incorporation of *Bapx* and *Gdf5/6/7* into a preexisting DV patterning program drove the evolution of the jaw by altering the identity of intermediate first-arch chondrocytes. We present this "Pre-pattern/Cooption" model as an alternative to current models linking the evolution of the jaw to the de novo appearance of sophisticated pharyngeal DV patterning.

vertebrate | jaw | evolution | pharynx | lamprey

The evolution of vertebrates from invertebrate chordates involved a shift from a lifestyle of passive filter feeding to one of active predation (1). This transition was marked by major changes to the structure of the pharynx, including the evolution of a robust pharyngeal skeleton composed of cellular cartilage. In the first vertebrates, this skeleton was simple, consisting of unjointed cartilaginous rods. In the lineage leading to gnathostome (jawed) vertebrates, these rods were modified to form distinct cartilages connected by specialized joint tissue. This arrangement is most conspicuous in the first arch, where articulating dorsal and ventral cartilages form the jaw. How the unjointed gill bars of the first vertebrates gave rise to the jointed gnathostome pharyngeal skeleton and jaws is an outstanding question in vertebrate evolution.

The gnathostome pharyngeal skeleton is derived exclusively from cranial neural crest cells (CNCCs) that migrate ventrally from the anterior neural tube into the pharynx. Once in the pharynx, these cells receive a variety of signals from surrounding tissues that regulate CNCC proliferation and pattern the nascent head skeleton (2, 3). Along the dorso-ventral (DV) axis, these signals drive the expression of several target genes, including the transcription factors *Hand*, *Msx*, *Dlx2,3,5,6*, *Goosecoid* (*Gsc*), *Barx*, and *Bapx*, and the secreted proteins *Gdf5* and *Chordin*. *Hand* and *Msx* are both expressed in nascent ventral cartilages (4, 5), whereas *Dlx* genes display nested expression patterns, with *Dlx3* expressed in an intermediate domain, *Dlx5,6* expression extending more dorsally, and *Dlx2* ubiquitously marking all DV domains (6–8). *Gsc* and *Barx* are expressed in discontiguous ventral and dorsal domains flanking the nascent joints in the first and second arches, whereas *Bapx*, *Gdf5*, and *Chordin* mark the nascent jaw joint in the intermediate domain of the first arch (5, 9).

Genetic perturbations in mouse, chick, and zebrafish have demonstrated that these genes interact with each other to determine the composition and shape of skeletal elements. In ventral arch skeletal primordia, a loss of *Hand* results in a loss of ventral arch cartilages, a loss of ventral *Gsc* expression, and a ventral expansion of *Bapx* (5). Loss of *Bapx* results in loss of *Gdf* and *Chordin* expression and elimination of the jaw joint itself (5), whereas combinatorial losses of *Dlx3,5*, and *6* result in various homeotic transformations in which ventral cartilages take on more dorsal identities (7, 8, 10).

Although many of the core genetic interactions that pattern the gnathostome pharyngeal skeleton and jaw have been described, it is unknown when these mechanisms first evolved in the vertebrate lineage or how they may have been altered during jaw evolution. An evolutionarily informative model for understanding the genetic changes underlying jaw evolution is the agnathan vertebrate lamprey. Lampreys are the most basal vertebrates amenable to experimental manipulations at embryonic stages. Like all vertebrates, lamprey has a pharyngeal skeleton made wholly or partially of neural crest-derived cellular cartilage (11–13). However, unlike jawed vertebrates, the lamprey pharyngeal skeleton consists of cartilage bars that fuse to form an unjointed branchial basket (Fig. S1). This unjointed arrangement is similar to that seen in the fossil agnathans (14, 15), and is thought to reflect the ancestral vertebrate condition.

Recent work suggests that the pharyngeal skeletons of agnathans and gnathostomes are patterned along the antero-posterior (AP) axis by largely conserved mechanisms. In both groups, cranial neural crest cells (CNCCs) destined to form the head skeleton migrate as three streams (the trigeminal, hyoid, and common branchial) at stereotyped AP positions (16, 17). Lamprey also displays gnathostome-like AP nesting of *Hox* expression in the pharynx, including a *Hox*-free first arch, a *Hox2*-expressing second arch, and *Hox2-8*-positive respiratory arches (18). Finally, in both lamprey and gnathostomes, the first arch and premandibular skeletons appear to be patterned by foci of *FGF8* and *BMP* signaling (19).

Although the core mechanisms for patterning the pharynx along the AP axis are conserved between jawed and jawless vertebrates, morphology and gene expression suggest differences in DV patterning between the two groups. In larval and adult lampreys, the branchial basket is virtually symmetrical along the

Author contributions: D.M.M. designed research; R.C., M.C., F.Y., and D.M.M. performed research; T.S.-S. and M.B.-F. contributed new reagents/analytic tools; R.C. and D.M.M. analyzed data; and D.M.M. wrote the paper.

The authors declare no conflict of interest.

Data deposition: The sequences reported in this paper have been deposited in the GenBank database (accession nos. HQ248098–HQ248103).

This article is a PNAS Direct Submission.

[1]To whom correspondence should be addressed. E-mail: Daniel.Medeiros@Colorado.edu.

This article contains supporting information online at www.pnas.org/lookup/suppl/doi:10.1073/pnas.1009304107/-/DCSupplemental.

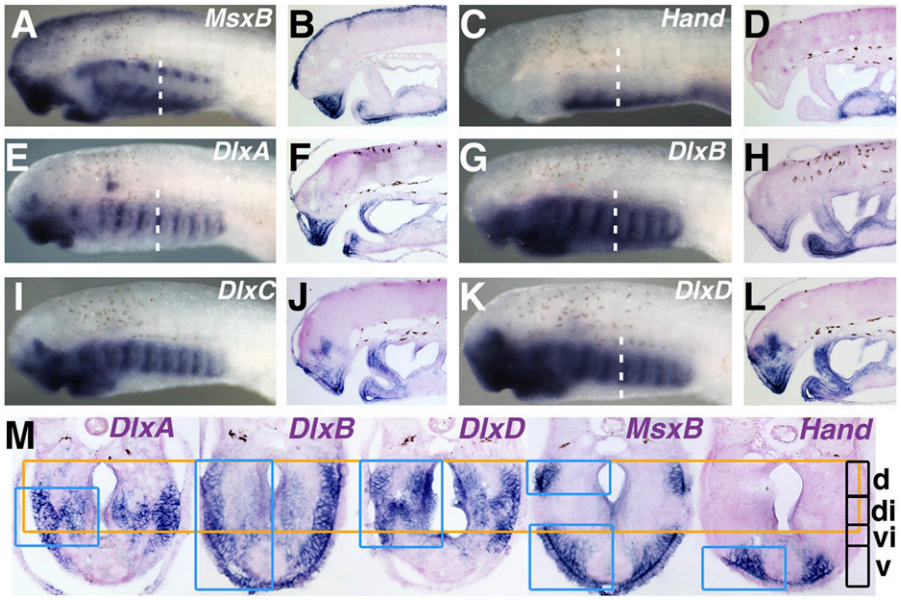

Fig. 1. Expression of *MsxB*, *Hand,* and *Dlx* genes in the larval lamprey head. All larvae are Tahara st. 26.5 and are shown in side view (*A, C, E, G, I,* and *K*), sagittal section (*B, D, F, H, J,* and *L*), and transverse section (*M*) (refer to Fig. S1 for a detailed description of larval lamprey pharyngeal morphology). (*A, C,* and *M*) *MsxB* expression in mesenchyme of the upper lip, lower lip, and ventral and dorsal pharynx. (*C, D,* and *M*) *Hand* expression in the ventral pharyngeal mesenchyme. (*E, F,* and *M*) *DlxA* expression around the mouth and in the pharyngeal arches. Expression in the lower lip is restricted to the posterior edge of the mouth. (*G, H,* and *M*) *DlxB* expression in the mesenchyme of the lower lip, pharyngeal arches, and surrounding the endostyle. Expression in the upper lip is reduced. (*I* and *J*) *DlxC* expression in ectoderm and mesenchyme of the upper and lower lips and in the pharyngeal arches. (*K, L,* and *M*) *DlxD* expression in the upper and lower lip, the pharyngeal arches, and overlying the endostyle. (*M*) Side-by-side comparison of *Dlx*, *Ms,x* and *Hand* expression along the DV axis in the pharynx at st. 26.5. Transverse sections through the dotted lines in *A, C, E, G,* and *K*. Sections were level matched to the fifth pharyngeal arch using the posterior limit of the endostyle as an internal reference point. Orange box serves as guide and bounds the pharyngeal cavity across all sections. Blue boxes define the DV extent of gene expression. DV expression of *DlxC* is similar to *DlxD* and is omitted for simplicity. Combinations of *Dlx*, *Msx*, and *Hand* genes mark four distinct DV domains. The ventral domain (v) expresses *DlxB*, *MsxB*, and *Hand*. Ventral intermediate (vi) domain expresses *DlxA,B,C,D,* and *MsxB*. The dorsal intermediate (di) domain expresses *DlxA,B,C,D*. Dorsal domain (d) expresses *DlxB,C,D,* and *MsxB*.

DV axis, with the morphology of its dorsal half mirroring that of its ventral half (19). In embryos, expression of lamprey *Dlx* genes has been reported throughout the DV extent of the pharyngeal arches (20–22), rather than in the nested pattern seen in gnathostomes (7). Intriguingly, loss of *Dlx* nesting in mouse results in agnathan-like DV symmetry in the first-arch skeleton (7, 10). These observations have led to speculation that the lamprey pharynx lacks significant DV patterning and that the evolution of such patterning was instrumental in the evolution of the jaw (7, 19, 20, 22).

Here we test the hypothesis that jaw evolution was driven by the evolution of sophisticated pharyngeal DV pattern, by examining the expression of lamprey homologs of gnathostome pharyngeal patterning genes. We observe nested *Dlx* gene expression in the lamprey head skeleton, as well as DV-restricted expression of *Hand, Msx*, and *Gsc*, revealing an unexpectedly high level of gnathostome-like DV pattern. In addition, we find that *Bapx*, a master regulator of jaw joint formation in gnathostomes, and *Gdf5*, its downstream target, are not expressed in the lamprey intermediate first arch, whereas *Barx*, which is excluded from the intermediate first arch in gnathostomes, marks this domain in lamprey. Taken together, these data support a model for gnathostome evolution in which the appearance of the jaw joint was driven by incorporation of *Bapx* and *Gdf5* into a sophisticated ancestral DV-patterning program. Based on gene expression in zebrafish mutants lacking jaw joints, and cell morphology in the lamprey head skeleton, we further propose that these cooptions potentiated jaw joint evolution by altering the fate of first-arch chondrocytes.

Results

Cloning and Expression of Lamprey *MsxA* and *MsxB*. A low-stringency library screen for *Msx* genes was performed using an arrayed embryonic *Petromyzon marinus* cDNA library (23). Two *Msx* paralogs were isolated. One corresponded to a previously described *Lethenteron japonicum Msx* gene, *LjMsxA*. The other was a previously uncharacterized *Msx* designated *MsxB* (Fig. S2). Like *LjMsxA*, *P. marinus MsxA* expression was most prominent in the upper lip ectoderm and mesenchyme at stage (st.) 25–28, with minor expression in the lower lip (Fig. S3). *MsxB* expression was first observed in the dorsal neural tube at neurula stages. Expression in the ventral pharynx began around st. 23 and expanded into the upper and lower lips at st. 25. This expression persisted until st. 26.5 (Fig. 1 *A, B,* and *M* and Fig. S3), when an addition dorsal pharyngeal domain was observed (Fig. 1 *A* and *M*). Sectioning revealed ventral pharyngeal expression was in mesenchyme surrounding the endostyle, the ventral-most aspect of the pharyngeal bars, and ventral ectoderm. Dorsal pharyngeal staining was also in pharyngeal mesenchyme/CNCC (Fig. 1*M*).

Cloning and Expression of Lamprey *Hand*. A single exon with high similarity to vertebrate *Hand* genes was identified in the preassembly *P. marinus* genome (Fig. S2) and used to design RACE primers and isolate a 5′ RACE product. *Hand* expression was first observed at st. 23 in the ventral pharynx. This pattern persisted until st. 26.5 (Fig. 1 *C, D,* and *M*). Sectioning showed that this expression was in mesenchyme underlying and flanking the endostyle. A medial stripe of *Hand* expression was also observed in the mesenchyme of the lower lip (ventral first arch) at st. 26.5 (Fig. S3).

Cloning and Expression of Lamprey *DlxA, DlxB, DlxC,* and *DlxD*. A low-stringency library screen for *Dlx* genes identified four *Dlxs* corresponding to the previously described *P. marinus* and *L. japonicum* paralogs, *DlxA*, *DlxB*, *DlxC*, and *DlxD* (20) (Fig. S4). Expression of all *Dlxs* in presumptive CNCC at st. 23–25 (Piavis

EVOLUTION

st. 14) was essentially as previously described (Fig. S5). At st. 26.5, we observed clear differences in *Dlx* paralog expression along the DV axis of the pharynx and around the mouth (Fig. 1 *E–M* and Fig. S6). *DlxA* expression was observed in the lower two-thirds of the posterior gill bars and was excluded from the mesenchyme around the endostyle (Fig. 1 *E, F,* and *M* and Fig. S6). In the oral region, *DlxA* marked the upper lip, the distal tip of the lower lip (ventral first arch) and the first-arch gill bar (Fig. 1 *E, F,* and *M* and Figs. S3 and S6). *DlxB* was expressed broadly throughout the pharyngeal mesenchyme/CNCC including the mesenchyme around the endostyle (Fig. 1 *G, H,* and *M* and Fig. S6). In the oral region, *DlxB* was strongest in the lower lip and was down-regulated in the medial portion of the upper lip (Fig. 1 *G, H,* and *M* and Figs. S3 and S6). *DlxC* expression was broader than *DlxA* but less extensive than *DlxB*, with expression throughout the DV extent of the gill bars and absent from the mesenchyme around the endostyle (Fig. 1 *I* and *J* and Fig. S6). In the oral region, strong *DlxC* expression was seen in the ectoderm and mesenchyme of the upper and lower lips (Fig. 1 *I* and *J* and Figs. S3 and S6). The DV extent of *DlxD* expression in the pharyngeal arches and around the mouth was similar to that of *DlxC* (Fig. 1 *K, L,* and *M* and Figs. S3 and S6). When considered in the context of *Msx* and *Hand* expression, unique combinations of *Dlx*, *MsxB,* and *Hand* were observed, marking four distinct DV domains of pharyngeal mesenchyme/CNCC: a $DlxB^{+}/Msx^{+}/Hand^{+}$ ventral domain, a $DlxA,B,C,D^{+}/MsxB^{+}$ ventral–intermediate domain, a $DlxA,B,C,D^{+}$ dorsal–intermediate domain, and a $DlxB,C,D^{+}/MsxB^{+}$ dorsal domain (Fig. 1*M*) in the posterior arches and around the mouth (Fig. S3).

Cloning and Expression of Lamprey *Goosecoid*. A single lamprey *Goosecoid* (*Gsc*) homolog was identified in the *P. marinus* EST database (Fig. S4). The cognate cDNA clone was isolated and used to make a riboprobe. *Gsc* expression was first observed in patches of upper lip mesenchyme and in pharyngeal endoderm at st. 25. By st. 26.5, *Gsc* expression in the upper lip mesenchyme had expanded and endodermal expression had resolved into a stripe of expression in the first pharyngeal pouch (Fig. 2 *A* and *B* and Fig. S3). Discontiguous expression of *Gsc* was seen in the first-arch mesenchyme, with transcripts detected in the gill bar and the distal tip of the lower lip (Fig. 2 *A* and *B*).

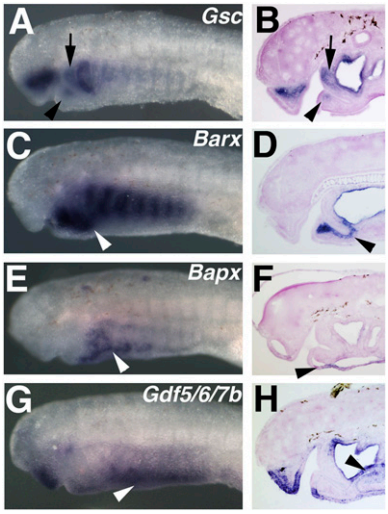

Fig. 2. Expression of lamprey *Gsc*, *Barx*, *Bapx*, and *Gdf5/6/7b* in the embryonic and larval head. All larvae are Tahara st. 26.5 and are shown in side view (*A, C, E,* and *G*) and sagittal section (*B, D, F,* and *H*). (*A* and *B*) *Gsc* expression in the mesenchyme of the upper lip, first-arch gill bar (arrow), and distal lower lip (arrowhead). (*C* and *D*) *Barx* expression in the mesenchyme of the lower lip, extending dorsally into the ventral portion of the first gill bar (arrowhead). (*E* and *F*) *Bapx* expression in the epidermis of the ventral pharynx (arrowhead). (*G* and *H*) *Gdf5/6/7b* expression in the upper and lower lip ectoderm, upper lip mesenchyme, pharyngeal endoderm, ventral ectoderm ,and ventral mesenchyme surrounding the endostyle (arrowhead).

Cloning and Expression of Lamprey *Barx*. Two exons of a single lamprey *Barx* gene were identified by searching the preassembly *P. marinus* genome using gnathostome *Barx* sequences (Fig. S4). These exons were amplified directly from genomic DNA and used to generate riboprobes. Lamprey *Barx* expression was first detected in two bilateral stripes in the lower lip at st. 25. By st. 26.5, *Barx* transcripts were detected in the presumptive CNCC medial to the mesoderm in every pharyngeal arch and strongly in the lower lip and velum (Fig. 2 *C* and *D* and Fig. S3). Parasagittal sections revealed a contiguous domain of expression in the first arch extending from the lower lip to the ventral portion of the gill bar (Fig. 2*D*).

Cloning and Expression of Lamprey *Bapx*. A single *Bapx* exon was identified in the preassembly *P. marinus* genome, and was used to design RACE primers and to isolate 5′ and 3′ RACE products (Fig. S7). *Bapx* expression was seen in the paraxial mesoderm, presumptive pronephros, and pharyngeal endoderm from st. 21–25 (Fig. S8). Beginning at st. 24, signal was observed in bilateral patches of ventral pharyngeal ectoderm (Fig. S8). This staining persisted until st. 26.5 (Fig. 2 *E* and *F* and Fig. S3).

Cloning and Expression of Lamprey *Gdf5/6/7a* and *Gdf5/6/7b*. The preassembly lamprey genome was searched for homologs of gnathostome *Gdf5*, a marker of joints in gnathostomes. Two 500- to 600-bp exons were identified, amplified directly from genomic DNA, and used to synthesize riboprobes and to screen an arrayed embryonic DNA for full-length clones. Phylogenetic analysis grouped the first with gnathostome *Gdf7* but with low confidence. The second was placed as an outgroup to gnathostome *Gdf5* and *Gdf6* paralogs at moderate bootstrap values (Fig. S7). To reflect the uncertain phylogeny, we designated the genes *Gdf5/6/7a* and *Gdf5/6/7b*. Expression of lamprey *Gdf5/6/7a* was seen throughout the head epidermis from st. 21 to st. 26.5 (Fig. S3). *Gdf5/6/7b* expression was first seen in the mesenchyme and ectoderm of the ventral pharynx and in two stripes of ectoderm flanking the preoral region at st. 23. These ectoderm patches fused anteriorly at st. 25–26.5, strongly marking the upper lip (Fig. 2 *G* and *H* and Fig. S3). Pharyngeal expression of *Gdf5/6/7b* persisted until st. 26.5 in the ventral ectoderm and mesenchyme flanking the endostyle (Fig. 2 *G* and *H*).

Discussion

Combinatorial Expression of *Dlx, Msx*, and *Hand* Define Four Distinct DV Domains in both Lamprey and Gnathostomes. Deep conservation of early neural crest developmental mechanisms (11, 12, 23) implies that jaw evolution was driven by later changes to the patterning of postmigratory cranial neural crest cells (CNCCs) and/or skeletogenic mesoderm. In gnathostomes, extracellular signals pattern the nascent pharyngeal skeleton by activating combinatorial expression of various target genes at specific DV levels. These factors then cooperate to confer positional identities upon nascent skeletal elements, determining their final shape and composition (2, 24). We examined the expression of lamprey homologs of the ventrally expressed patterning genes *Msx* and *Hand* in the lamprey pharynx. Consistent with a conserved role in specifying ventral CNCC, we observed lamprey *MsxB* in the ventral aspect of the pharyngeal bars and *Hand*/*MsxB* coexpression in the lower lip and mesenchyme surrounding the endostyle (Fig. 1).

Nested expression of *Dlx2,3,5,6* has been shown to confer DV identities upon pharyngeal CNCC in both mouse and zebrafish (6, 7, 25), suggesting that this mechanism evolved before the

divergence of lobe-finned and ray-finned fish. Previous reports describe ubiquitous expression of four *Dlx* paralogs in the pharynx of *P. marinus* and the Japanese lamprey *Lethenteron japonicum* at early larval stages (Tahara st. 25/Piavis st. 14, 12–13 d postfertilization), before the pharyngeal arches have fully formed. These results led to speculation that a pharyngeal *Dlx* code is a gnathostome novelty associated with the evolution of the jaw (7, 19, 20, 22). Because of the clear DV restriction of *Hand* and *Msx* in later larvae, we decided to revisit lamprey *Dlx* gene expression at st. 26.5 (15–16 d postfertilization). At this stage, pharyngeal arch formation is complete and pharyngeal CNCCs have condensed into prechondrogenic rods. Recent work has shown that the full *Dlx* code does not resolve until similar late-pharyngula stages in gnathostomes (8, 26). As with *Msx* and *Hand*, we used a high-stringency in situ hybridization protocol and level-matched transverse sections to accurately compare the extent of *Dlx* paralog expression along the DV axis. With these methods, we found clear differences in the expression of *P. marinus Dlx* paralogs, with different combinations of *Dlxs* marking distinct DV domains in the upper lip, first arch, and posterior arches (Fig. 1). Notably, these results differ from previous reports of uniform *Dlx* expression throughout the pharyngeal CNCC in *P. marinus* and *L. japonicum*. Although staging and methodological differences likely explain these discrepancies, it is formally possible that they reflect independent evolution of nested *Dlx* expression in *P. marinus*, or the loss of such patterning in *L. japonicum*. Despite a recent divergence time of 10–30 million years ago for the two species (27), differences in gene expression between them have been suggested (18, 28).

In jawed vertebrates, combinatorial expression of *Dlxs*, *Msx*, and *Hand* define four distinct DV domains of pharyngeal CNCC. Recent work in zebrafish has refined this map (8), revealing a $Dlx2^{+}$/Msx^{+}/$Hand^{+}$ ventral domain, a $Dlx2,3,5,6^{+}$ ventral-intermediate domain, a $Dlx2,5,6^{+}$ dorsal-intermediate domain, and a $Dlx2^{+}$ dorsal domain. This code diverges slightly in the first arch, with expression of *Dlx5,6* extending into the ventral domain. We found that, as in gnathostomes, combinatorial expression of *Msx, Hand,* and *Dlxs* in lamprey also defines four DV domains. These include a $DlxB^{+}$/Msx^{+}/$Hand^{+}$ ventral domain, a $DlxA,B,C,D^{+}$/$MsxB^{+}$ ventral-intermediate domain, a $DlxA,B,C,D^{+}$ dorsal-intermediate domain, and a $DlxB,C,D^{+}$/$MsxB^{+}$ dorsal domain. Furthermore, as in gnathostomes, lamprey displays alterations to this code in the first arch, with the expression of intermediate *Dlx* paralogs *(DlxC, D)* extending ventrally. Although strikingly gnathostome-like, we also noted agnathan-specific divergence of the pharyngeal *Dlx*/*Msx*/*Hand* code. In gnathostomes, only *Dlx2* marks the dorsal-most domain, whereas three *Dlx* genes and *Msx* mark this domain in lamprey. In addition, *DlxA* expression in the lamprey first arch has extended dorsally and become discontiguous, marking separate domains in the dorsal and ventral first arch (first gill bar and lower lip, respectively). Despite these differences, the most parsimonious explanation for the existence of a gnathostome-type pharyngeal *Dlx*/*Msx*/*Hand* code in lamprey is that such patterning was present in the common ancestor of jawed and jawless vertebrates. This ancestral pattern then diverged in one or both lineages during the half-billion years separating lamprey and gnathostomes.

Conservation of a gnathostome-type pharyngeal *Dlx*/*Msx*/*Hand* code in lamprey requires that some of the gene duplications that produced the gnathostome *Dlx* paralogs occurred in the first vertebrates. The six gnathostome *Dlx* genes were created by tandem duplication of an ancestral *Dlx gene*, followed by two whole-genome duplications and gene loss. These events produced three pairs of linked genes (*Dlx1,2*, *Dlx3,4*, and *Dlx5,6*), with each pair including members of two *Dlx* subfamilies (*Dlx1,4,6* and *Dlx2,3,5*). Phylogenetic analyses (20, 22, 29) (Fig. S4) group lamprey *DlxA,B,C* within the *Dlx2,3,5* subfamily, but fail to support placement of *DlxD* within either gnathostome *Dlx* subfamily. Neighbor-joining analysis provides some support for a *DlxB*/*Dlx2* clade (Fig. S4) that is consistent with the broad *Dlx2*-like expression observed for lamprey *DlxB*. However, there is no support for one-to-one orthology between any other lamprey and gnathostome *Dlx*. Taken together, the tenuous phylogenetic positions of lamprey *Dlxs* leave open the precise relationships between agnathan and gnathostome *Dlx* paralogs. This may be due to the rapid evolution of lamprey genes relative to their gnathostome homologs (27). Assembly of the lamprey genome and identification of conserved vertebrate synteny groups should help to establish the timing of the duplications that generated the gnathostome and lamprey *Dlx* paralogs.

DV Patterning in the Lamprey Pharynx Correlates with Different Skeletal Cell Types. In gnathostomes, combinatorial expression of *Dlx*, *Msx,* and *Hand* is thought to perform two related patterning functions. Initially, it confers positional identities on pharyngeal CNCC, instructing cells at intermediate levels to differentiate into joint tissue, and those at dorsal and ventral levels to form cartilage. Later, it instructs nascent cartilages to take on level-specific morphologies (8). The lamprey head skeleton lacks both joint tissue and individual cartilages with level-specific morphologies. This lack of overt patterning raises the question of why the lamprey pharynx displays such sophisticated patterns of gene expression along its DV axis. Recent and historical accounts suggest that, despite DV symmetry in the branchial basket, the larval lamprey head skeleton varies in cellular composition along its DV axis. Schaffer (30) and others (31, 32) describe a skeletal tissue consisting of mesenchymal cells embedded in a stiff extracellular matrix termed "mucocartilage" in the ventral-most pharynx (Fig. S1). This tissue surrounds the endostyle and sits ventral to the definitive cartilage of the branchial basket. Modern dye-labeling (11) and gene expression (12) suggests that mucocartilage mesenchyme is derived from CNCC. Recent work has also revealed differences in the morphology of branchial basket chondrocytes (33), with those in the gill bars displaying a highly ordered "stack of coins" morphology, those in the dorsal-most horizontal (subchordal) cartilage bars appearing polygonal in shape, and those in the ventral-most horizontal (hypobranchial) cartilage bars forming irregular stacks. Furthermore, these populations likely form from separate dorsal, ventral, and intermediate chondrogenic condensations (34). Thus, the larval lamprey pharyngeal skeleton consists of at least four distinct CNCC-derived skeletal cell types positioned at specific DV levels: mesenchymal mucocartilage, hypobranchial chondrocytes, gill bar chondrocytes, and subchordal chondrocytes. Interestingly, the positions of these cell types correspond well to four domains of combinatorial *Dlx*, *MsxB,* and *Hand* expression identified in this study (Fig. 3). These data suggest that the ancestral function of pharyngeal DV patterning may have been to specify skeletal cell types and morphologies at different DV levels within the pharyngeal arches. This system was then used to position joint tissue and to regulate the shape of nascent cartilages in the gnathostome lineage.

First-Arch Expression of the Jaw Joint Regulators *Bapx* and *Gdf5/6/7* Is Unique to Gnathostomes. Like the posterior arches, the gnathostome first arch is patterned by combinatorial expression of *Dlx*, *Msx*, and *Hand* transcription factors. Gnathostome-like expression of these genes in lamprey suggests that this patterning is an ancestral feature of vertebrate pharyngeal arch development. Superimposed upon this *Dlx*/*Msx*/*Hand* DV code, the gnathostome first arch has additional patterning distinguishing it from the posterior arches. This includes discontiguous expression of *Gsc* and *Barx* in the dorsal and ventral aspects of the first arch, focal expression of *Bapx* and *Gdf5* in the intermediate domain that gives rise to the jaw joint, and ventral expression of *Dlx5,6* (5, 9). These patterning add-ons constitute potential novelties associated with specialization of the first arch into the jaw.

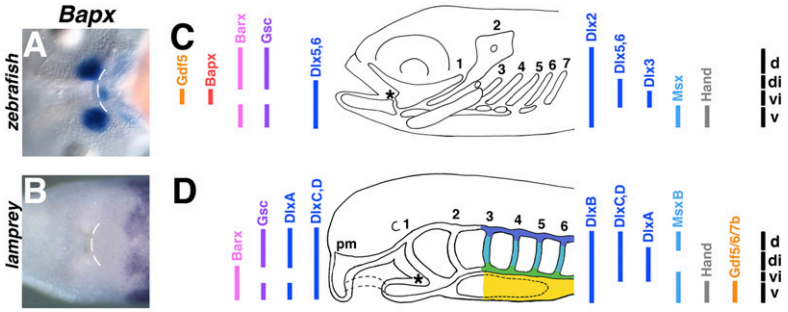

Fig. 3. Comparison of DV patterning gene expression in the developing zebrafish and lamprey pharyngeal skeletons. (*A*) Ventral view of a 48hpf zebrafish embryo showing *Bapx* expression flanking the mouth in the forming jaw joints. (*B*) Lamprey *Bapx* expression is never observed in the nascent head skeleton. Dotted line marks the posterior edge of the mouth in both *A* and *B*. (*C*) DV extent of *Gdf5*, *Bapx*, *Barx*, *Gsc, Dlx2,3,5,6*, *Msx*, and *Hand* in the pharyngeal arches of the zebrafish. First-arch–specific patterning is depicted by the colored bars to the left of the diagram. Asterisk marks the jaw joint. (*D*) DV extent of *Barx*, *Gsc, DlxA,B,C,D*, *Msx*, *Hand,* and *Gdf5/6/7b* in the pharyngeal arches of the sea lamprey. First-arch–specific patterning is depicted by the colored bars to the left of the diagram. In both zebrafish and lamprey, combinatorial expression of *Dlx*, *Msx*, and *Hand* genes defines four domains of CNCC in the pharynx; ventral (v), ventral-intermediate (vi), dorsal-intermediate (di), and dorsal (d), suggesting sophisticated DV patterning is a basal feature of vertebrate head skeleton development. Although lamprey possesses a region topologically homologous to the jaw joint (asterisk), as indicated by similar first-arch–specific expression of *Dlx, Msx, Hand,* and *Gsc,* first-arch expression of *Gdf5* and *Bapx* appears to be unique to gnathostomes, suggesting that recruitment of these genes to the first arch was associated with the evolution of the jaw. Combinatorial expression of lamprey *Dlx*, *Msx*, and *Hand* in the posterior pharynx corresponds to four distinct skeletal cell types, namely, mucocartilage (yellow), hypobranchial chondrocytes (green), "stack-of-coins" gill bar chondrocytes (light blue), and subchordal chondrocytes (dark blue). Pm, premandibular mesenchyme.

To test when these features of first-arch patterning evolved, we examined expression of *Gsc, Barx, Gdf5,* and *Bapx* in lamprey larvae. The lamprey first arch is part of a highly specialized oral skeleton derived from both premandibular and first arch CNCC (35) (Figs. S1 and S3). Although very different from the gnathostome jaw, recent work has defined the contribution of the first arch to the lamprey oral skeleton, facilitating comparisons between the lamprey and gnathostome first arch (19, 35, 36). We found that, as in gnathostomes, lamprey *Gsc* marks discontiguous dorsal and ventral domains in the presumptive first arch. These domains overlap with ventral *Dlx, Msx,* and *Hand* expression in the lower lip and dorsal *Dlx* expression in the pharyngeal gill bar, and flank a *Gsc*-free intermediate domain between the lower lip and first gill bar. Taken together, these data suggest topological homology between the intermediate first arch in lamprey and the gnathostome jaw joint, and support evolution of first-arch–specific patterning early in the vertebrate lineage (Fig. 3).

In contrast to *Gsc*, we did not find gnathostome-like expression of *Barx*, *Bapx*, or *Gdf5/6/7* in the lamprey first arch. Instead, we observed contiguous expression of *Barx* in the lower lip and intermediate first arch, and no *Gdf5/6/7* or *Bapx* expression in the presumptive CNCC of any pharyngeal arch. These findings are particularly provocative, as *Bapx* loss-of-function in gnathostomes leads to a loss of *Gdf5* expression and fusion of the maxillary and mandibular cartilages (5), whereas a loss of *Gdf5/6/7* function results in the widespread loss of joints in the axial and appendicular skeletons (37). In addition, zebrafish *furinA* and *plc3βc* mutants, which lack intermediate first arch *Bapx* expression, have fused first-arch cartilages, and display contiguous first-arch *Barx* expression (9), reminiscent of the agnathan condition. These results suggest that a gain of *Bapx* and *Gdf5/6/7* expression in the gnathostome first arch was associated with the evolution of the jaw joint.

It is unclear what the consequences of *Bapx and Gdf5/6/7* cooption to the intermediate first arch may have been. *Bapx* labels intermediate first arch CNCCs that form the jaw joint in nonmammalian gnathostomes (5) and the homologous joint between the malleus and incus in mammals (38). *Bapx* knockdown in zebrafish causes a loss of the jaw joint and jaw joint-specific expression of *Gdf5* and *Chordin* in zebrafish (5). However, first-arch *Bapx* expression in zebrafish is broader than the joint, including nascent chondrocytes in the upper and lower jaws (5). Furthermore, in mouse, *Bapx* knock-out causes a reduction in the size of the inner ear bones but does not effect the malleus-incus joint or joint-specific expression of *Gdf5/6*(38). *Bapx* knockdown also does not effect the formation joints in the posterior pharyngeal arches or elsewhere in the axial or appendicular skeletons of fish or mouse (5, 39). Taken together these data suggest that *Bapx* likely performs a first-arch–specific patterning function rather than a joint-specification function. In this context, it is unlikely *Bapx* cooption alone was a driving force in the evolution of the jaw joint; rather, novel expression of *Bapx* in the intermediate first arch likely served to reinforce or refine first-arch DV pattern in early gnathostomes.

In contrast to *Bapx*, members of the *Gdf5/6/7* paralogy group are general markers of joint tissue in gnathostomes (5, 40, 41). Loss of *Gdf5* and/or *Gdf6* results in the loss of joints as well as in reduced growth of bones and cartilages, suggesting that *Gdf5/6/7* plays roles in both joint specification and cartilage growth (40–42). In lamprey, *Gdf5/6/7b* is expressed in patches of pharyngeal ectoderm and endoderm, as well as in the mucocartilage of the ventral pharynx (Fig. 2). Interestingly, classical and modern descriptions of mucocartilage suggest it shares several features with the *Gdf5/6/7*-expressing hyaline cartilage found in gnathostome joints (31). Both tissues consist of scattered secretory cells embedded in a matrix of hyaluronic acid, chondroitin sulfate, and microfibrils, and both are surrounded by a collagenous perichondrium. It is possible that novel expression of *Gdf5/6/7* may have driven the formation of mucocartilage-like joint tissue in the intermediate first arch of the gnathostome ancestor.

Prepattern/Cooption Model of Vertebrate Jaw Evolution. Aspects of pharyngeal arch patterning conserved in agnathans and gnathostomes can reasonably be expected to have been present in their last common ancestor. Based on similar expression of *Dlx, Msx, and Hand* in the pharynx, we propose that the last common ancestor of jawed and jawless vertebrates deployed these genes to pattern its pharynx along the DV axis. This pattern was sophisticated, dividing the pharyngeal CNCC into at least four domains specified by various combinations of *Dlx, Msx*, and *Hand* genes, and giving rise to distinct types of skeletal tissue (Fig. 3). This basal pattern was likely present in all pharyngeal arches, although the first arch displayed some additional pattern including discontiguous domains of *Gsc* expression, and ventral expansion of some *Dlx* paralogs. From this ancestral state, the

lamprey and gnathostome patterns diverged, with changes to the DV boundaries of particular *Dlx* and *Msx* genes in one or both lineages. In gnathostomes, *Bapx* was coopted to the intermediate first-arch domain, disrupting ancestrally contiguous *Barx* expression and augmenting or refining the ancestral DV pattern. Subsequent recruitment of *Gdf5/6/7* to this domain then drove the evolution of the jaw joint, possibly by conferring mucocartilage-like properties upon nascent first-arch chondrocytes.

Our model is based on the assumptions that features present only in gnathostomes constitute gnathostome novelties, whereas similarities between lamprey and gnathostomes reflect shared, derived features of vertebrates. However, it is also possible that gnathostome-specific features such as first-arch *Bapx* expression are the result of evolutionary loss in the lamprey lineage. Similarly, putatively conserved features such as nested *Dlx* expression could formally reflect parallel evolution from an ancestor lacking pharyngeal DV pattern. Critical tests of these alternate scenarios will be the expression of pharyngeal DV patterning genes in elasmobranchs and hagfish. Recent molecular phylogenies suggest that hagfish are derived agnathan vertebrates related to lampreys (29, 43), and progress has been made in obtaining hagfish embryos (44). Gnathostome-like expression of *Dlx, Msx,* and *Hand* in hagfish would confirm that a pharyngeal *Dlx/Msx/Hand* code is a basal feature of vertebrate development. First-arch expression of *Bapx* and *Gdf5/6/7* in elasmobranchs, but not agnathans, would suggest that these aspects of first-arch patterning are indeed gnathostome synapomorphies, as predicted by our model.

Materials and Methods

Low and moderate stringency library screens for *Msx, Dlx*, and *Gdf5/6/7* genes were performed as previously described (23). *Barx*, *Gdf5/6/7a*, and *Gdf5/6/7b* exons were PCR amplified from adult lamprey genomic DNA according to standard methods. All other genes were isolated from embryonic cDNA using the GeneRacer kit (Invitrogen). In situ hybridizations were performed as previously described (16) with some modifications. For details, see *SI Materials and Methods*.

ACKNOWLEDGMENTS. We thank Roger Bergstedt, Deborah Winkler, Nikolas Rewald, and Kathy Jones (Hammond Bay Biological Station, Millersburg, MI) for generously supplying adult lampreys; Gage Crump and David Stock for critical reading of the manuscript; and two anonymous reviewers whose comments helped improve this work. R.C. was supported by the Grant Agency of the Academy of Sciences of the Czech Republic (206/07/P257) and by Ministry of Education, Youth, and Sports Project 0021620828. M.C. and D.M.M. were supported by National Science Foundation Grant IOS0920751 (to D.M.M.). T.S.-S. was supported by National Institutes of Health Grant DE017911 (to M.B.-F.).

1. Gans C, Northcutt RG (1983) Neural crest and the origin of vertebrates: A new head. *Science* 220:268–273.
2. Clouthier DE, Schilling TF (2004) Understanding endothelin-1 function during craniofacial development in the mouse and zebrafish. *Birth Defects Res C Embryo Today* 72:190–199.
3. Walshe J, Mason I (2003) Fgf signalling is required for formation of cartilage in the head. *Dev Biol* 264:522–536.
4. Thomas T, et al. (1998) A signaling cascade involving endothelin-1, dHAND and msx1 regulates development of neural-crest-derived branchial arch mesenchyme. *Development* 125:3005–3014.
5. Miller CT, Yelon D, Stainier DY, Kimmel CB (2003) Two endothelin 1 effectors, hand2 and bapx1, pattern ventral pharyngeal cartilage and the jaw joint. *Development* 130: 1353–1365.
6. Walker MB, Miller CT, Coffin Talbot J, Stock DW, Kimmel CB (2006) Zebrafish furin mutants reveal intricacies in regulating Endothelin1 signaling in craniofacial patterning. *Dev Biol* 295:194–205.
7. Depew MJ, Lufkin T, Rubenstein JLR (2002) Specification of jaw subdivisions by Dlx genes. *Science* 298:381–385.
8. Talbot JC, Johnson SL, Kimmel CB (2010) hand2 and Dlx genes specify dorsal, intermediate and ventral domains within zebrafish pharyngeal arches. *Development* 137:2507–2517.
9. Walker MB, Miller CT, Swartz ME, Eberhart JK, Kimmel CB (2007) phospholipase C, beta 3 is required for Endothelin1 regulation of pharyngeal arch patterning in zebrafish. *Dev Biol* 304:194–207.
10. Jeong J, et al. (2008) Dlx genes pattern mammalian jaw primordium by regulating both lower jaw-specific and upper jaw-specific genetic programs. *Development* 135: 2905–2916.
11. McCauley DW, Bronner-Fraser M (2003) Neural crest contributions to the lamprey head. *Development* 130:2317–2327.
12. McCauley DW, Bronner-Fraser M (2006) Importance of SoxE in neural crest development and the evolution of the pharynx. *Nature* 441:750–752.
13. Langille RM, Hall BK (1988) Role of the neural crest in development of the trabeculae and branchial arches in embryonic sea lamprey, *petromyzon marinus* (L). *Development* 102:301–310.
14. Shu DG, et al. (2003) Head and backbone of the Early Cambrian vertebrate *Haikouichthys*. *Nature* 421:526–529.
15. Gess RW, Coates MI, Rubidge BS (2006) A lamprey from the Devonian period of South Africa. *Nature* 443:981–984.
16. Meulemans D, Bronner-Fraser M (2002) Amphioxus and lamprey AP-2 genes: Implications for neural crest evolution and migration patterns. *Development* 129: 4953–4962.
17. Cerny R, et al. (2004) Developmental origins and evolution of jaws: New interpretation of "maxillary" and "mandibular". *Dev Biol* 276:225–236.
18. Takio Y, et al. (2007) Hox gene expression patterns in Lethenteron japonicum embryos—insights into the evolution of the vertebrate Hox code. *Dev Biol* 308: 606–620.
19. Shigetani Y, Sugahara F, Kuratani S (2005) A new evolutionary scenario for the vertebrate jaw. *Bioessays* 27:331–338.
20. Neidert AH, Virupannavar V, Hooker GW, Langeland JA (2001) Lamprey Dlx genes and early vertebrate evolution. *Proc Natl Acad Sci USA* 98:1665–1670.
21. Myojin M, et al. (2001) Isolation of Dlx and Emx gene cognates in an agnathan species, Lampetra japonica, and their expression patterns during embryonic and larval development: Conserved and diversified regulatory patterns of homeobox genes in vertebrate head evolution. *J Exp Zool* 291:68–84.
22. Kuraku S, Takio Y, Sugahara F, Takechi M, Kuratani S (2010) Evolution of oropharyngeal patterning mechanisms involving Dlx and endothelins in vertebrates. *Dev Biol* 341:315–323.
23. Sauka-Spengler T, Meulemans D, Jones M, Bronner-Fraser M (2007) Ancient evolutionary origin of the neural crest gene regulatory network. *Dev Cell* 13:405–420.
24. Charité J, et al. (2001) Role of Dlx6 in regulation of an endothelin-1-dependent, dHAND branchial arch enhancer. *Genes Dev* 15:3039–3049.
25. Robinson GW, Mahon KA (1994) Differential and overlapping expression domains of Dlx-2 and Dlx-3 suggest distinct roles for Distal-less homeobox genes in craniofacial development. *Mech Dev* 48:199–215.
26. Kimmel CB, Ballard WW, Kimmel SR, Ullmann B, Schilling TF (1995) Stages of embryonic development of the zebrafish. *Dev Dyn* 203:253–310.
27. Kuraku S, Kuratani S (2006) Time scale for cyclostome evolution inferred with a phylogenetic diagnosis of hagfish and lamprey cDNA sequences. *Zoolog Sci* 23: 1053–1064.
28. Cohn MJ (2002) Evolutionary biology: Lamprey Hox genes and the origin of jaws. *Nature* 416:386–387.
29. Kuraku S, Meyer A, Kuratani S (2009) Timing of genome duplications relative to the origin of the vertebrates: Did cyclostomes diverge before or after? *Mol Biol Evol* 26: 47–59.
30. Schaffer J (1896) Uber das knorpelige skelett von Ammocoetes branchialis nebst Bemerkungen ueber das knorpelgewebe in Allgemeienen. *Z Wiss Zool* 61:606–615.
31. Wright GM, Youson JH (1982) Ultrastructure of mucocartilage in the larval anadromous sea lamprey, Petromyzon marinus L. *Am J Anat* 165:39–51.
32. Gaskell WH (1908) *The Origin of Vertebrates* (Longmans, Green, and Co., London).
33. Martin WM, Bumm LA, McCauley DW (2009) Development of the viscerocranial skeleton during embryogenesis of the sea lamprey, Petromyzon Marinus. *Dev Dyn* 238:3126–3138.
34. Morrison SL, Campbell CK, Wright GM (2000) Chondrogenesis of the branchial skeleton in embryonic sea lamprey, Petromyzon marinus. *Anat Rec* 260:252–267.
35. Shigetani Y, et al. (2002) Heterotopic shift of epithelial-mesenchymal interactions in vertebrate jaw evolution. *Science* 296:1316–1319.
36. Takio Y, et al. (2004) Evolutionary biology: Lamprey Hox genes and the evolution of jaws. *Nature* 429:262.
37. Settle SH, et al. (2003) Multiple joint and skeletal patterning defects caused by single and double mutations in the mouse Gdf6 and Gdf5 genes. *Dev Biol* 254:116–130.
38. Tucker AS, Watson RP, Lettice LA, Yamada G, Hill RE (2004) Bapx1 regulates patterning in the middle ear: Altered regulatory role in the transition from the proximal jaw during vertebrate evolution. *Development* 131:1235–1245.
39. Tribioli C, Lufkin T (1999) The murine Bapx1 homeobox gene plays a critical role in embryonic development of the axial skeleton and spleen. *Development* 126: 5699–5711.
40. Settle SH, Jr. et al. (2003) Multiple joint and skeletal patterning defects caused by single and double mutations in the mouse Gdf6 and Gdf5 genes. *Dev Biol* 254: 116–130.
41. Storm EE, Kingsley DM (1999) GDF5 coordinates bone and joint formation during digit development. *Dev Biol* 209:11–27.
42. Storm EE, Kingsley DM (1996) Joint patterning defects caused by single and double mutations in members of the bone morphogenetic protein (BMP) family. *Development* 122:3969–3979.
43. Stock DW, Whitt GS (1992) Evidence from 18S ribosomal RNA sequences that lampreys and hagfishes form a natural group. *Science* 257:787–789.
44. Ota KG, Kuraku S, Kuratani S (2007) Hagfish embryology with reference to the evolution of the neural crest. *Nature* 446:672–675.